Transient outward current contributes to Wenckebach-like rhythms in isolated rabbit ventricular cells

ALI R. YEHIA, ALVIN SHRIER, KIRK C.-L. LO, AND MICHAEL R. GUEVARA
Department of Physiology, McGill University, Montreal, Quebec, Canada H3G 1Y6

Yehia, Ali R., Alvin Shrier, Kirk C.-L. Lo, and Michael R. Guevara. Transient outward current contributes to Wenckebach-like rhythms in isolated rabbit ventricular cells. *Am. J. Physiol.* 273 (*Heart Circ. Physiol.* 42): H1–H11, 1997.— Wenckebach-like rhythms in isolated rabbit ventricular cells are characterized by beat-to-beat increments in action potential duration (APD) and latency, giving rise to a beat-to-beat decrease in the recovery interval and culminating in a skipped beat. These systematic APD changes are associated with a beat-to-beat decrease in the slope of the early repolarizing phase (*phase 1*) of the action potential, which is partially controlled by the transient outward potassium current (I_{to}). When I_{to} is blocked with 4-aminopyridine, periodic Wenckebach rhythms are replaced by aperiodic Wenckebach rhythms, in which the beat-to-beat changes in the slope of *phase 1* and in APD disappear but the beat-to-beat increase in latency remains. A beat-to-beat decrease in I_{to}, parelleling the beat-to-beat changes in the slope of *phase 1* and in APD, is seen in action-potential clamp experiments with Wenckebach rhythms previously recorded in the same cell. Simulations with an ionic model of I_{to} show cyclical changes in I_{to} consistent with the experimental data. These results demonstrate a key role for I_{to} in the generation of maintained periodic Wenckebach rhythms in isolated rabbit ventricular cells.

action-potential clamp; 4-aminopyridine; excitability; ionic currents; ionic model

PRECEDING EACH SYNCHRONIZED CONTRACTION of the ventricles of the heart, ventricular cells develop an action potential in response to a depolarizing current generated by activation of their upstream neighbors. A perfectly normal cell will cease to respond in this 1:1 fashion to the input current when the time between input stimuli becomes too short or when the effective stimulus strength becomes too small. There will then be a transition from 1:1 to some other rhythm (e.g., 2:1 block, complete block, alternans, Wenckebach rhythm). In this article we focus on the transition to Wenckebach rhythm, which has been described classically at the level of the atrioventricular (AV) node. In AV nodal Wenckebach, there is a progressive beat-to-beat slowing of conduction velocity within the AV node, culminating in a single skipped ventricular beat, after which the cycle repeats (38, 44, 45). However, Wenckebach rhythms have also been described in virtually all other areas of the heart (see Ref. 18 for references), including ventricular muscle (2).

The mechanism most commonly invoked to account for the blocked beat is decremental conduction, in which there is a progressive diminution of the amplitude, maximum upstroke velocity, and conduction velocity of the action potential of the blocked beat as it traverses the conduction pathway (19, 44). However, Wenckebach-like rhythms have recently been observed in single cells isolated from the AV node (1, 25) and in single ventricular cells (11, 12, 20), both of which preparations show no sign of spontaneous activity, as well as in spontaneously beating aggregates of embryonic chick ventricular cells (22) and in single cells isolated from the sinoatrial node (3). It is highly unlikely that mechanisms involving conduction, such as decremental conduction, would play a role in generating Wenckebach rhythms in these isopotential preparations.

Previous studies in isolated guinea pig ventricular cells have attributed the generation of Wenckebach rhythms to a complex interplay between the delayed rectifier, inward rectifier, and fast sodium currents, leading to a beat-to-beat increase in latency (11, 12). This in turn produces a beat-to-beat decrease in recovery time, which eventually results in a dropped beat when the refractory period is sufficiently encroached on (11, 12). However, in single rabbit ventricular cells, the dropped beat is preceded by beat-to-beat increases in action potential duration (20). Because these increments are much larger than concomitant beat-to-beat increases in latency (20), they are predominantly responsible for producing beat-to-beat decrements in recovery time. In this paper we demonstrate that the transient outward current, I_{to}, which is not present in guinea pig ventricular cells (40), is responsible for producing the beat-to-beat increase in action potential duration seen during Wenckebach rhythm in rabbit ventricular myocytes and for regularizing the rhythm. Preliminary results of this work have been presented in abstract form (46).

MATERIALS AND METHODS

Cell isolation techniques. New Zealand White rabbits of either sex were used (1.8–2.4 kg). After intramuscular administration of 150 mg ketamine (Ketaset, Wyeth-Ayerst, Montreal, Canada) and 20 mg xylazine (Rompun, Haver, Etobicoke, Canada), 5,000 U of heparin (Hepalean, OrganoTeknika, Toronto, Canada) were injected into an ear vein. After the animal was given a blow to the back of the neck, the heart was quickly removed and mounted on a Langendorff perfusion apparatus. The coronary bed was perfused in the retrograde direction through the aorta with normal Ca^{2+} solution for ~5 min (see *Solutions*) and then with low-Ca^{2+} solution for ~10 min. The perfusion was continued for another 5 min with low-Ca^{2+} solution to which 165 U/ml of collagenase type XI (Sigma) had been added. Protease type XIV (0.23 U/ml, Sigma) was then added to the previous mixture, and perfusion was continued for an additional 3 min before the heart was removed and placed in a vessel containing the protease-collagenase solution at 37°C for 8–15 min. All the above perfusion solutions were warmed (35–37°C) and gassed with 95% O_2-5% CO_2 throughout the isolation procedure, setting the pH to ~7.2. The right ventricular wall was then cut free

and transferred to modified Kraftbrühe (KB) solution (see *Solutions*) at room temperature (22–24°C). After the solution was gently stirred, chunks of tissue were discarded, leaving a clear suspension containing isolated rod-shaped ventricular cells, which was then placed in the refrigerator (8°C). Procedures involving animals were approved by the University's Animal Care Committee (NIH assurance no. A5006-01) and conformed to the requirements of the Canadian Council on Animal Care and the *Guide for the Care and Use of Laboratory Animals* [DHHS Publication No. (NIH) 85–23, Revised 1985, Office of Science and Health Reports, Bethesda, MD 20892].

Electrophysiological techniques. Aliquots of the suspension were transferred to a chamber mounted on the stage of an inverted microscope. After settling to the bottom of the bath, the cells were superfused with *N*-2-hydroxyethylpiperazine-*N'*-2-ethanesulfonic acid (HEPES)-buffered bath solution (see *Solutions*), which was bubbled with 100% O_2. Only Ca^{2+}-tolerant cells showing clear cross striations were used. Glass suction microelectrode pipettes (2.5–3.5 MΩ) were fabricated with a vertical puller (PP-83, Narishige Scientific Instruments, Tokyo, Japan) and filled with pipette solution (see *Solutions*). A hydraulic micromanipulator (MO-103M, Narishige Scientific Instruments) was used to place the microelectrode tip in contact with the cell membrane. Gentle mouth suction allowed the formation of a gigaohm seal and subsequent disruption of the membrane patch. An amplifier (Axoclamp 2A, Axon Instruments, Foster City, CA), bridge-balanced and capacity compensated, was used in bridge or continuous single-electrode voltage-clamp mode. An 80386-based computer equipped with a 12-bit analog-to-digital (A/D) card (DAS-20, Omega Engineering Stamford, CT) was used to carry out voltage-clamp and action-potential clamp (AP clamp) protocols, which were run on-line with the Patch-kit program (version 1.0, Alembic Software, Montreal, Canada). Signals were also recorded on a video cassette recorder after A/D conversion at 22 kHz (Neuro-Corder DR-484, Neuro Data Instruments, New York, NY) for later off-line analysis (data were then sampled at 1–5 kHz with appropriate anti-alias filtering). Experiments were conducted at 34–36°C or at 22–24°C.

In AP clamp experiments, the membrane potential waveform was stored on tape and then replayed, and a segment containing several action potentials was selected. This segment was then sampled at a rate of 1–5 kHz, with appropriate anti-alias filtering, and was stored in a disk file on the microcomputer. The stored trace was held in a circular buffer, reconverted back to an analog signal (with a 12-bit digital-to-analog converter), and applied repetitively in the same cell as the command signal for the voltage-clamp amplifier. To compensate for a slight drift (typically 1–2 mV) in the membrane potential of the cell that occurred during the time between the initial recording of the action potential and the application of the AP clamp in control conditions (typically 5 min), we adjusted the holding potential on the amplifier so that the resting potential of the AP clamp trace coincided to within 1 mV with the current resting potential of the cell (27). Although in theory no current should have been injected by the amplifier when the cell was clamped by its own activity in control conditions (27), in practice small deflections were usually seen (see e.g., Fig. 1*B* of Ref. 37). When a specific current is then blocked, the amplifier injects a current to compensate for the blocked current, thus providing a measurement of the contribution of that current to the action potential during control (i.e., no block) conditions.

Any drift in action potential properties causes artifactual current to appear in the AP clamp current record, because the clamp then injects a current to compensate for this change in the currents generated by the cell. Because action potential morphology drifted faster at higher bath temperatures, presumably because of faster rundown of currents, all AP clamp experiments were conducted at room temperature to minimize the drift that inevitably occurs during the delay (15–20 min) between recording and selecting the action potential series, applying control AP clamp, admitting the blocker to the bath, and, finally, applying AP clamp for a second time.

Solutions. The normal-Ca^{2+} solution contains (in mmol/l) 121 NaCl, 5 KCl, 1 $MgCl_2$, 2.8 sodium acetate, 15 $NaHCO_3$, 5.5 glucose, and 2.2 $CaCl_2$ (17). The low-Ca^{2+} solution has the same composition as normal-Ca^{2+} solution but with no added $CaCl_2$. The bath solution contains (in mmol/l) 121 NaCl, 5 KCl, 1 $MgCl_2$, 2.8 sodium acetate, 10 HEPES, 10 glucose, and 2.2 $CaCl_2$ at pH 7.4 (adjusted with NaOH) (17). The modified KB solution contains (in mmol/l) 85 KCl, 5 $MgSO_4$, 30 K_2HPO_4, 20 glucose, 0.5 ethylene glycol-bis(β-aminoethyl ether)-*N*,*N*,*N'*,*N'*-tetraacetic acid (EGTA), 5 Na_2ATP, 5 sodium pyruvate, 5 creatinine, 20 taurine, 11.4 sodium succinate, 5 β-OH-butyric acid, and 25 g/l polyvinylpyrrolidone-40 at pH 7.3 (adjusted with KOH) (28). The pipette solution contains (in mmol/l) 140 KCl, 1 $MgCl_2$, 5 HEPES, 1.54 $CaCl_2$, 5 EGTA, and 5 Na_2ATP at pH 7.0 (adjusted with KOH).

RESULTS

Wenckebach-like rhythms. With the temperature kept constant at a value between 34 and 36°C, injection of a train of suprathreshold current pulses (10-ms duration, >500-pA amplitude) at a basic cycle length (BCL) of 300 ms into an isolated myocyte resulted in a 1:1 rhythm (i.e., one action potential for each stimulus pulse). When the pulse amplitude was then gradually decreased from this suprathreshold level, an occasional skipping or dropping of an action potential ("beat") occurred. Further decreases in the stimulus pulse amplitude in steps of <1 pA produced rhythms containing Wenckebach cycles. An $n + 1$:n Wenckebach cycle consists of $n + 1$ injected stimuli giving rise to n action potentials and one dropped beat. Figure 1*A* (*top*) shows a regular train of 3:2 Wenckebach cycles that was interrupted by one 2:1 cycle (sixth cycle). The pulse amplitude remained constant during stimulation (Fig. 1*A*, *bottom*). We refer to the rhythm in Fig. 1*A* as a periodic Wenckebach rhythm, because it consists of a series of consecutive Wenckebach cycles, each containing the same number of action potentials. In contrast, an aperiodic form of Wenckebach rhythm, which will be encountered later, consists of successive Wenckebach cycles that do not contain the same number of action potentials.

Use of the term Wenckebach implies that there is a monotonic beat-to-beat trend in at least one of the parameters describing the action potential. Figure 1*B* shows superimposed action potentials isolated from the fourth 3:2 cycle that follows the 2:1 cycle in Fig. 1*A*, illustrating a beat-to-beat increase in the action potential duration (APD) measured from the overshoot of the action potential to 90% repolarization (APD_{90}). The diastolic interval (DI) of a particular action potential is

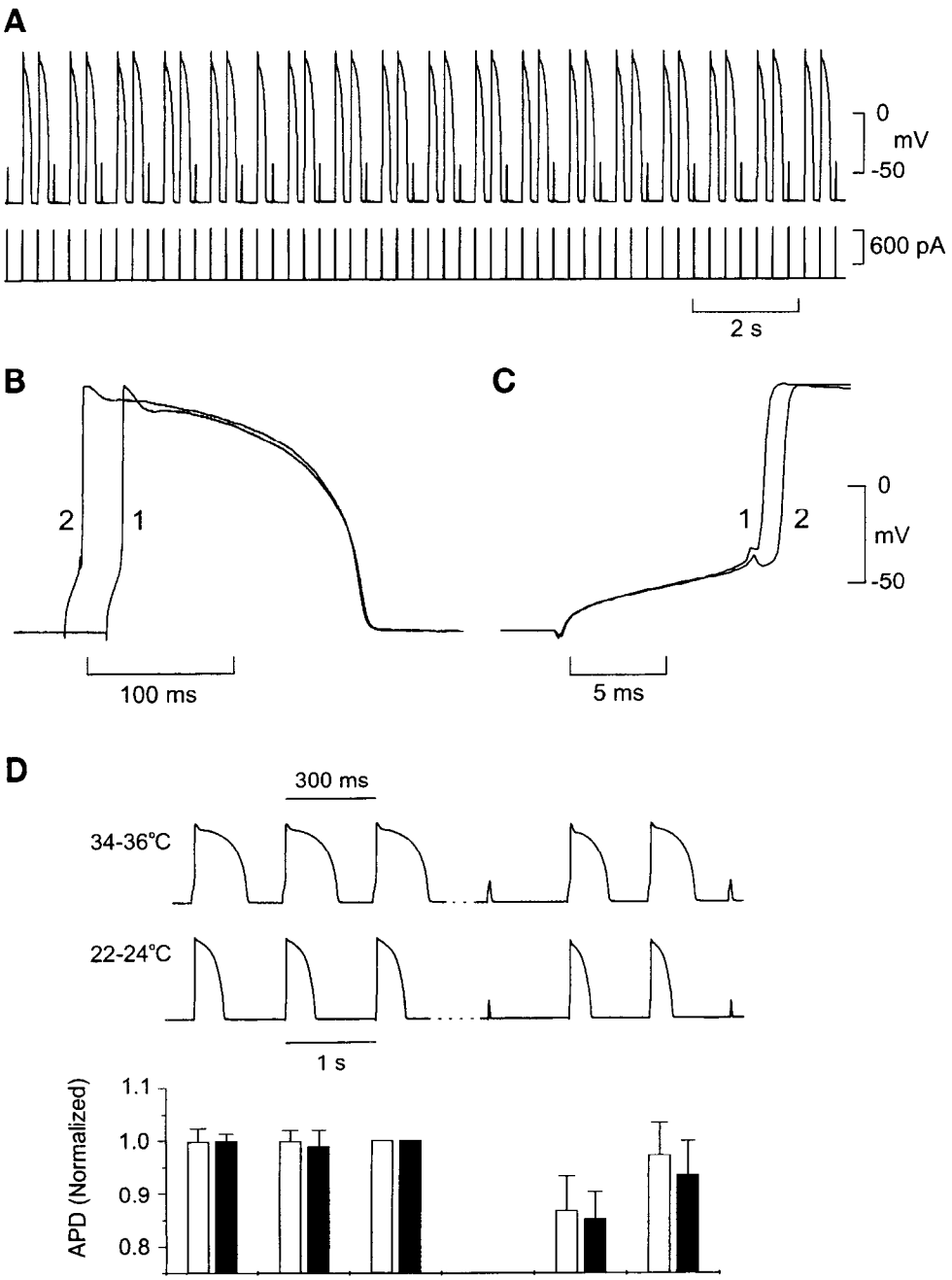

Fig. 1. Wenckebach-like rhythm in an isolated ventricular myocyte. *A, top*: transmembrane potential showing a series of 3:2 Wenckebach cycles interrupted by a single 2:1 cycle (6th cycle); *bottom*: stimulus pulse train, with basic cycle length (BCL) = 300 ms, pulse amplitude = 900 pA, pulse duration = 10 ms. All data at 34–36°C unless indicated otherwise. *B*: action potentials (*action potential 1* and *action potential 2*) from 4th 3:2 cycle after 2:1 cycle in *A*, superimposed with respect to *phase 3*, showing beat-to-beat increase in action potential duration (APD) from 163 to 183 ms. *C*: upstroke phases for same cycle, showing beat-to-beat increase in latency from 10.8 to 11.8 ms. *D, top*: 3 consecutive action potentials taken from 1:1 rhythm (*left*) and 2 action potentials from a 3:2 Wenckebach cycle (*right*) at 34–36°C (BCL = 300 ms) and 22–24°C (BCL = 1,000 ms); *bottom*: APD (means ± SD) normalized to APD of 3rd beat of 1:1 rhythm shown for each cell (open bars, 9 cells at 34–36°C; solid bars, 8 cells at 22–24°C).

defined as the time from 90% repolarization of the immediately preceding action potential to the time at which the overshoot of the action potential in question occurred. The longest DI of the Wenckebach cycle was thus for the first action potential of the cycle. There was also a concomitant beat-to-beat increase in latency, defined as the time between the onset of the injected current pulse and the time at which maximal upstroke velocity occurred (Fig. 1*C*). These changes in latency were much smaller than the changes in APD and were comparable to those found in guinea pig myocytes with 10-ms duration stimulus pulses (Fig. 2*C* of Ref. 12). Traces similar to those shown in Fig. 1 were obtained in eight other cells (resting potential = −76.3 ± 1.9 mV, mean ± SD; n = 9). Wenckebach rhythms could also be produced by decreasing BCL, thereby keeping stimulus amplitude constant (20).

The sequence of three action potentials in Fig. 1*D* (*top left*) was taken from a period of 1:1 rhythm at a suprathreshold pulse amplitude. The two action potentials at the *top right* are from a 3:2 Wenckebach cycle obtained in the same cell, but at a lower pulse amplitude. As with isolated guinea pig ventricular myocytes studied in the whole cell recording mode (43), there was considerable cell-to-cell variability in the APD of rabbit cells during 1:1 rhythm. We thus normalized the APD of the action potentials in Fig. 1*D* to the APD of the third action potential of the 1:1 rhythm. The bars (Fig. 1*D*,

bottom) give the APD (mean ± SD, n = 9 cells) normalized in such a fashion for each cell. The APD of the first and second beats of the Wenckebach cycle were 13% (normalized APD = 0.87 ± 0.066) and 3% (normalized APD = 0.97 ± 0.062) shorter than the APD during 1:1 rhythm. A Student's t-test between the APD of either of the first two action potentials of the 1:1 sequence and the APD of the first action potential of the 3:2 Wenckebach cycle showed that they were significantly different ($P < 0.0002$). However, the same test with the second action potential of the Wenckebach cycle showed that its APD was not significantly different from the APD during 1:1 rhythm.

Effect of lowering temperature on Wenckebach rhythms. Although Wenckebach rhythms can be produced in multicellular Purkinje strands by focal cooling (15), they are not seen in normal tissue at more physiological temperatures where there is a direct transition from 1:1 rhythm to 2:1 block (8). Figure 1*D* shows that Wenckebach rhythms were found at a longer BCL (1,000 ms) in experiments conducted at room temperature (22–24°C) than at 34–36°C (BCL = 300 ms), which is in keeping with the longer APD and refractory period at 22–24°C. However, within a Wenckebach cycle, the relative beat-to-beat change in APD was preserved (compare filled and open bars at bottom of Fig. 1*D*). At 22–24°C the latency tended to be longer, the maximal upstroke velocity was lower, and it was easier to obtain higher order (e.g., 4:3) Wenckebach cycles. In addition, periodic 3:2 Wenckebach rhythms were less common than at 34–36°C (Fig. 1*A*); instead, one tended to obtain rhythms consisting of, for example, mixtures of 3:2 and 4:3 Wenckebach cycles.

Effect of intentionally dropping a beat. During a Wenckebach cycle, in addition to beat-to-beat increments in APD, there were almost always beat-to-beat increments in latency (Fig. 1*C*). To investigate whether the increase in latency itself might have any direct causal effect on the increase of the subsequent APD, we conducted experiments in which a cell was driven at a BCL of 300 ms with a suprathreshold pulse amplitude at 34–36°C. A single stimulus pulse was then deliberately dropped from the pulse train (Fig. 2*A*). At this high pulse amplitude, there were no beat-to-beat increases in the latency of the action potentials on resumption of stimulation. Yet, the first action potential after the resumption of stimulation (*action potential 4* in Fig. 2*B*) had an APD that was shorter than that of the action potential just before the stimulus was dropped (*action potential 3*). The second action potential after resumption of stimulation (*action potential 5*), although also shorter in duration than the control action potential (*action potential 3*), was not as short as the first action potential (*action potential 4*). Figure 2*C* shows the results (means ± SD) from 10 cells in which APD was normalized to the APD of *action potential 3* in each cell. On average, there was a decrease of ~14% (normalized APD = 0.86 ± 0.046) in the APD of the first beat elicited after stimulation was resumed after the pause, which was comparable to the value of 13% observed for the first beat during Wenckebach rhythm at 34–36°C (Fig. 1*D*). A Student's t-test showed that the APD of *beat 4* ($P < 0.00005$) or *5* ($P < 0.05$) was significantly different from the APD of *beat 1* or *2* (Fig. 2*C*). Figure 2*D* shows that the decrease in APD for *action potential 4* was seen in each of the 10 cells, despite considerable cell-to-cell variability in the APD of *action potential 3*. Similar results were obtained at 22–24°C, with the mean normalized APD (n = 12 cells) being 88% of the control value on the first beat after resumption of stimulation at BCL = 1,000 ms, compared with 86% at 34–36°C (Fig. 2*C*).

Because there was no beat-to-beat increment in latency for the action potentials after the resumption of stimulation in Fig. 2*A* (latency was 11 ms for all 8 beats), a beat-to-beat increment in latency is not necessary to have a beat-to-beat increment in APD. In addition, the absence of a subthreshold response in Fig.

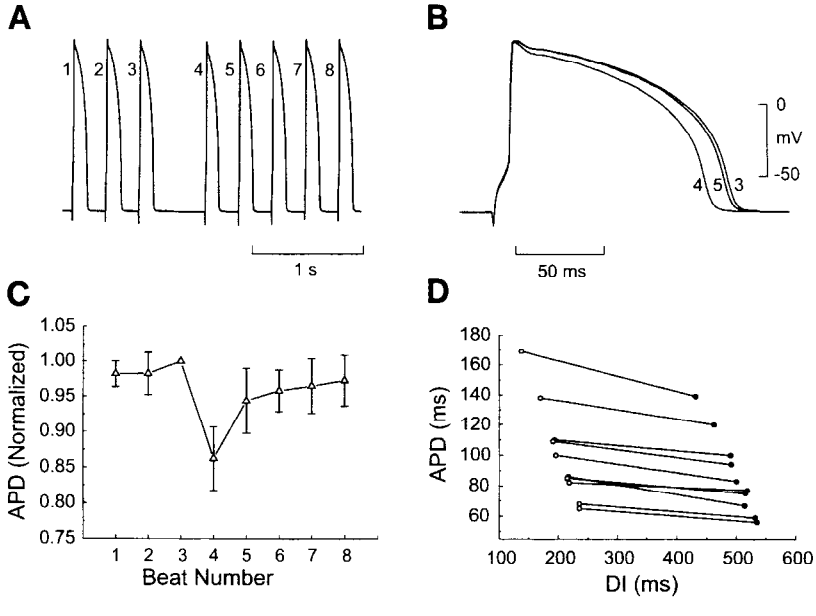

Fig. 2. Intentional omission of a single stimulus pulse during 1:1 rhythm. *A*: cell driven at BCL = 300 ms with a suprathreshold pulse amplitude of 828 pA (10-ms duration). A single stimulus pulse is omitted. *B*: superimposition of last action potential before stimulus was omitted (*action potential 3*) together with first 2 action potentials after skipped stimulus (*action potentials 4* and *5*). APD = 126, 114, 124 ms, respectively. *C*: APD (means ± SD) normalized to APD of last beat before skipped stimulus for each cell (△, n = 10 cells). *D*: APD of *beats 3* (○) and *4* (●) plotted against corresponding diastolic interval (DI) for all 10 cells. Downward deflections preceding action potentials in *A* and *B* are stimulus artifacts caused by imperfect bridge balance. Temperature: 34–36°C.

2*A* demonstrates that this response is not necessary to obtain the beat-to-beat increments in APD after a dropped beat.

Slow recovery from inactivation of I_{to}. The action potentials in Fig. 1*B* are superimposed relative to *phase 3* of the action potential. This demonstrates that the beat-to-beat changes in APD were largely caused by changes during the early repolarization phase of the action potential (*phase 1*), which was steeper for the first action potential of the cycle and more shallow for the second action potential. Because I_{to} is known to act in the early phase of repolarization (17) and has been associated with a steepening of *phase 1* (4, 16, 40), we decided to investigate the role of this current in generating Wenckebach rhythms.

I_{to} has a relatively slow time-dependent recovery from inactivation (4, 17, 24). Figure 3*B* (*inset*) shows the paired-step voltage-clamp protocol used to investigate the time dependence of recovery from inactivation. The membrane was held at −80 mV, and a first step (P1) to +60 mV (close to the reversal potentials of Na^+ and Ca^{2+} to minimize Na^+ and Ca^{2+} currents) was imposed for a duration of 5 s to completely inactivate I_{to}. The membrane was then returned to the −80 mV holding potential for a variable recovery time (RT) before a second step (P2) to +60 mV was imposed (duration = 2 s) to assess the degree of recovery from inactivation of I_{to}. The membrane was held at −80 mV for 10 s between the end of one P2 step and the beginning of the subsequent P1 step. Figure 3*A* shows that as RT became longer, the peak I_{to} elicited by the second step became larger, demonstrating time-dependent recovery from inactivation. Peak unsubtracted current (mean, n = 5 cells) elicited by P2 is plotted against RT in Fig. 3*B* after being normalized for each cell to the peak unsubtracted current elicited by the immediately preceding P1 conditioning pulse. The data were well fit by a single exponential curve with a time constant of 882 ms (Fig. 3*B*), which agrees with prior work demonstrating the relatively slow kinetics of recovery from inactivation of I_{to} in rabbit ventricle at 33–35°C (24). At 22–24°C, the time constant for recovery from inactivation of I_{to} is much longer (mean = 7.2 s for 6 cells), which again agrees with a prior report of 5.7 s (17).

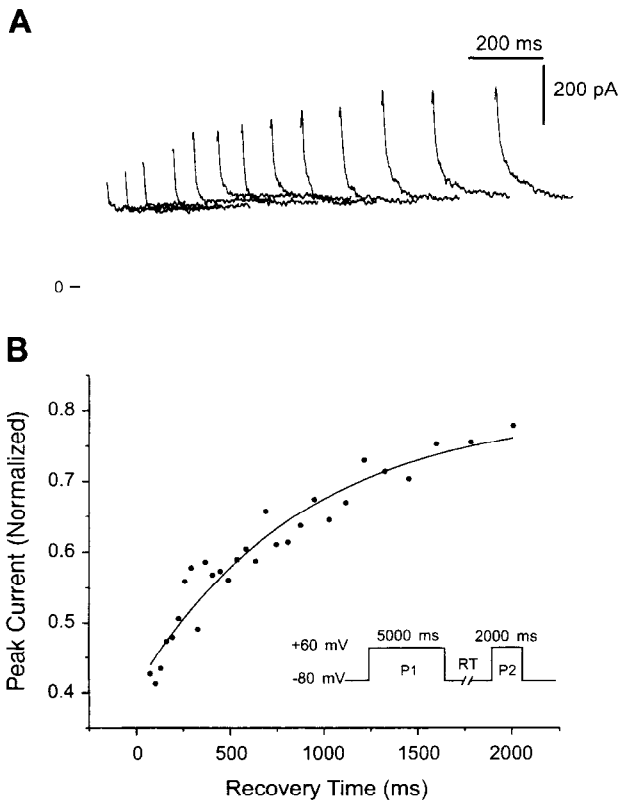

Fig. 3. Slow recovery from inactivation of transient outward current (I_{to}). *B*, *inset* shows protocol: from a holding potential of −80 mV, 2 steps (P1, P2) are made to +60 mV with durations of 5 s (P1) and 2 s (P2), separated by an exponentially increasing recovery time (RT). *A*: current traces during 2nd clamp step (P2) showing time-dependent recovery of I_{to}. First trace is for RT = 75 ms and last trace is for RT = 2,004 ms. *B*: peak normalized I_{to} vs. RT. Mean unsubtracted value obtained from 5 cells is plotted after being normalized to unsubtracted peak current elicited by conditioning (P1) step at each trial (minimal SD = 0.06, maximal SD = 0.35). Plot is well fit by a single-exponential curve with a time constant of 882 ms. Peak unsubtracted current at minimal RT is nonzero because of presence of instantaneous jump in clamp current at onset of clamp step. Temperature: 34–36°C.

During a 3:2 Wenckebach rhythm at a BCL of 300 ms, the DI associated with the first beat is ~400–550 ms, whereas that of the second beat is ~125–250 ms (see also Fig. 2*D*). From Fig. 3*B*, it is apparent that the magnitude of the normalized peak I_{to} after a RT of 500 ms is greater than that after a RT of 250 ms. Thus the relatively long time constant for recovery from inactivation of I_{to} would result in significantly more outward current flow during the first beat of a Wenckebach cycle than during the second beat, serving to shorten the APD of the first beat.

Effect of 4-aminopyridine on Wenckebach cycles. To investigate the role of I_{to} in generating Wenckebach rhythms, we blocked I_{to} with 2 mmol/l 4-aminopyridine (4-AP), at which concentration there is virtually complete block of I_{to} in single rabbit ventricular cells (17, 24, 41). Figure 4*A* shows superimposed action potentials from a 3:2 cycle taken during control conditions (*top*) and after application of 4-AP (*bottom*). Not only was the APD of both beats of the 3:2 cycle lengthened by 4-AP but also the characteristic beat-to-beat increments in APD within the 3:2 cycle (Fig. 4*A*, *top*) disappeared, and the configuration of action potentials within the 3:2 cycle became much more uniform. In fact, in the particular 3:2 cycle depicted in Fig. 4*A* (*bottom*), the APD of the second beat was shorter than that of the first beat. Similar results were seen in three other cells at 34–36°C and in five cells at 22–24°C.

Figure 4*B* (*top*) shows APD for a series of eight consecutive action potentials recorded during 1:1 rhythm in control conditions, whereas Fig. 4*C* (*top*) shows APD for several consecutive 3:2 Wenckebach cycles in the same cell, also in control conditions. The beat-to-beat increments in APD during the Wenckebach cycles (Fig. 4*C*, *top*) were greater than the spontaneous beat-to-beat fluctuations in APD during 1:1 rhythm (Fig. 4*B*, *top*). In addition, beat-to-beat incre-

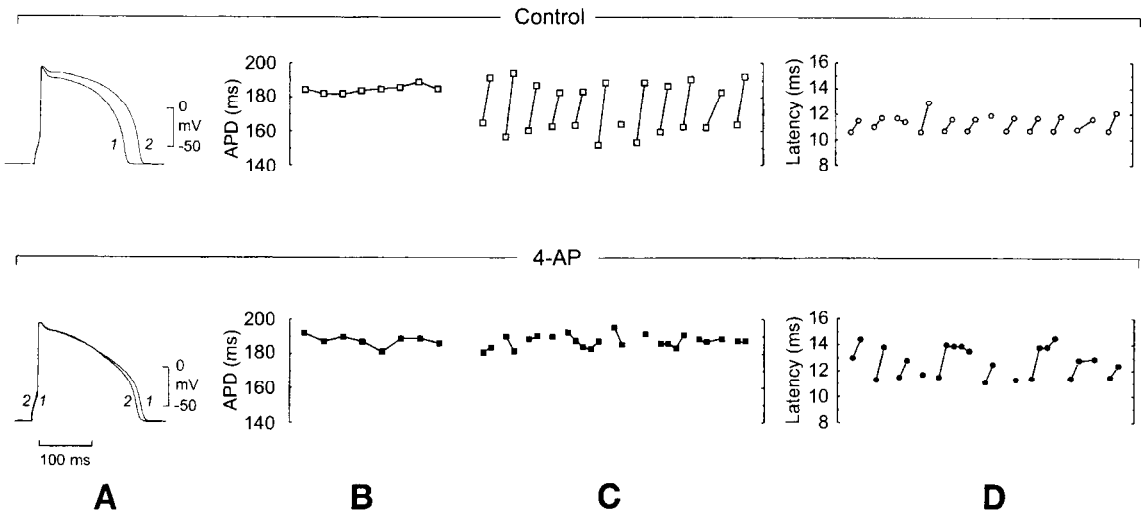

Fig. 4. Effect of block of I_{to} with 2 mmol/l 4-aminopyridine (4-AP). *Top*: control conditions (open symbols); *bottom*: 4-AP (solid symbols). *A*: superimposed action potentials from 3:2 cycle taken from run from which data in *C* are a subset. *B*: beat-to-beat changes in APD for 8 consecutive beats during 1:1 rhythm. *C*: beat-to-beat changes in APD during Wenckebach rhythm. Scale in *B* applies to *C*. *D*: beat-to-beat changes in latency during Wenckebach rhythm. Data points in *C* and *D* from same uninterrupted sequence of action potentials. Temperature: 34–36°C.

ments in latency (Fig. 4*D*, *top*) were associated with these increments in APD, with one exception (a decrement of latency associated with an increment in APD during the third 3:2 cycle). With the addition of 4-AP (2 mmol/l), it became impossible to produce periodic Wenckebach rhythms. Instead, we obtained aperiodic Wenckebach rhythms that still retained the beat-to-beat increments in latency (Fig. 4*D*, *bottom*) but lost the parallel beat-to-beat increments in APD (Fig. 4*C*, *bottom*). The APD fluctuated in an apparently random fashion from beat to beat but stayed within the range normally observed during 1:1 rhythm under 4-AP (Fig. 4*B*, *bottom*).

Figure 4 also points out the central role of DI in producing periodic Wenckebach rhythms in control. We define the recovery interval associated with a stimulus pulse as the time between 90% repolarization of the action potential immediately preceding the stimulus and the beginning of the stimulus itself. The recovery interval preceding the second beat of the 3:2 cycles in control (Fig. 4*C*, *top*) was 124–137 ms, whereas the recovery interval preceding the skipped beat was much shorter (94–104 ms). Despite a decrease in latency during the third Wenckebach cycle in Fig. 4*D* (*top*), a skipped beat resulted, presumably because the increment in APD (Fig. 4*C*, *top*) produced a sufficiently large decrement in recovery interval. In contrast, during exposure to 4-AP (Fig. 4*C*, *bottom*), the role of recovery interval was not crucial, because there was overlap in the range of the recovery interval between consecutive action potentials and the range of the recovery interval associated with the skipped beat (94–106 and 97–105 ms, respectively).

Action-potential clamp experiments. The AP clamp approach (14, 27, 37) was used to determine the time course of the 4-AP-sensitive current during Wenckebach rhythms. Experiments were conducted at 24–26°C to minimize the effect of drift (see MATERIALS AND METHODS). A cell was first stimulated in current-clamp mode to obtain Wenckebach rhythms. Figure 5*A* shows three successive action potentials of a 4:3 Wenckebach cycle superimposed relative to *phase 3*. Imposing this rhythm back on the cell with the use of the AP clamp under control conditions resulted only in small artifactual deflections in the membrane current (see MATERIALS AND METHODS). In the presence of 4-AP (2 mmol/l), when the same 4:3 Wenckebach rhythm was imposed under AP clamp, a relatively large transient current was revealed during the early repolarizing phase of the action potential (Fig. 5*B*). This current underwent a beat-to-beat decrease as the Wenckebach cycle progressed that is consistent with a beat-by-beat accumulation of inactivation of I_{to}. Similar responses were seen in five other cells.

The upward humps appearing toward the end of the traces in Fig. 5*B* were commonly seen. These humps do not vary in morphology as the Wenckebach cycle progresses and therefore cannot play any role in the genesis of the beat-to-beat changes characteristic of a Wenckebach cycle. Moreover, a small change in holding potential (~2 mV) modified the magnitude and even changed the direction of the hump, with virtually no change in the appearance of the larger early transient deflections.

Modeling. To investigate whether our present understanding of I_{to} (obtained from voltage-clamp experiments) might be sufficient to account for the AP clamp trace of Fig. 5*B*, we formulated an ionic model of I_{to} and investigated its response to room-temperature AP clamp (see APPENDIX for equations). As described above, Fig. 5*A* shows three superimposed action potentials from a 4:3 Wenckebach cycle, whereas Fig. 5*B* shows traces of the corresponding 4-AP-sensitive current recorded in the same cell during AP clamp. Figure 5*C* shows the I_{to} traces from the ionic model during simulated AP clamp, driven with the same voltage waveform as in Fig. 5*A*,

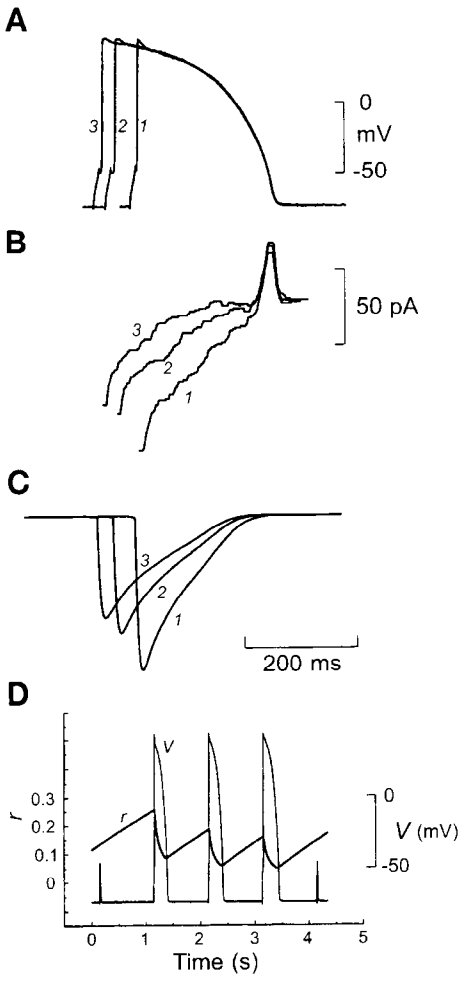

Fig. 5. Action potential clamp (AP clamp). *A*: superimposed action potentials from experimentally obtained 4:3 Wenckebach cycle used to conduct AP clamp in cell and in model. *B*: superimposed current traces from AP clamp performed on cell with 2 mmol/l 4-AP showing beat-to-beat decrease in I_{to} during Wenckebach rhythm. *C*: I_{to} from model simulation during AP clamp. *D*: voltage (V) and inactivation variable of I_{to} (r) during AP clamp simulation. Time constants for inactivation and recovery from inactivation of I_{to} used in simulation (*C* and *D*) were measured in same cell from which recordings in *A* and *B* were taken. See APPENDIX for model equations. Time scale in *C* applies to *A* and *B*; current scale in *B* applies to *C*. Temperature: 24–26°C.

revealing a time course of I_{to} similar to that seen in the experimental trace. Figure 5*D* shows the time course of r, the inactivation variable of I_{to}, superimposed on the voltage waveform used to drive the model. The r variable has a staircaselike waveform, showing that there is a beat-to-beat accumulation of inactivation as the Wenckebach cycle proceeds. It is this treppe phenomenon that is essentially responsible for the beat-to-beat changes in I_{to} seen in the model (Fig. 5*C*). This behavior would also presumably account for the fact that the shortening of the APD of the beat immediately after an intentionally dropped stimulus at 24–26°C was slightly less than that of the first beat of a 3:2 Wenckebach cycle (12 vs. 15%), because there would have been a slightly greater accumulation of inactivation during a maintained 1:1 rhythm than during a maintained 3:2 rhythm.

DISCUSSION

Ionic mechanisms underlying Wenckebach cycles in single rabbit ventricular cells. As a Wenckebach cycle progresses in the absence of 4-AP, there is a gradual beat-to-beat change in the morphology of the action potential, culminating in a skipped beat. Associated with this change in morphology are monotonic trends in the parameters describing the action potential; e.g., there are beat-to-beat increases in latency and APD, whereas there are beat-to-beat decreases in maximal upstroke velocity (at 22–24°C) and the slope of *phase 1* repolarization (Figs. 1; 4*C*, *top*; and 5, *A* and *D*). Because the Wenckebach phenomenon is cyclic, it is difficult to arrive at firm conclusions as to cause and effect. For example, the beat-to-beat decrease in maximal upstroke velocity seen at 22–24°C is almost certainly causally connected with the beat-to-beat increase in latency, because, as latency increases (to as long as 20 ms), the membrane spends an increasingly longer time at a depolarized potential (during the foot of the action potential), thus increasing the inactivation of the fast inward sodium current (I_{Na}) and slowing the subsequent upstroke velocity. However, there is no direct evidence to suggest any cause-and-effect relationship between the changes in latency and APD (Fig. 2).

Combined experimental and modeling work in guinea pig ventricular cells has suggested that the beat-to-beat increase in latency is produced by a complex mechanism involving an interplay among the time-dependent deactivation of the delayed rectifier current (I_K), the recovery from inactivation of I_{Na}, and the voltage-dependent conductance of the inward rectifier current (I_{K1}) (11, 12). A crucial component in this scenario is the relatively long time constant of deactivation of I_K at the resting potential (11, 12). It was subsequently shown that I_K in guinea pig ventricle is actually composed of two components, I_{Kr} and I_{Ks} (35). The more rapidly deactivating component, I_{Kr}, rectifies and is blocked specifically by E-4031, whereas the slower component, I_{Ks}, is linear, E-4031 insensitive, and larger in amplitude than I_{Kr}. Because the time constant of deactivation of I_{Kr} at rest is very short in the guinea pig (~50 ms) (35), it is virtually certain that it is the much slower I_{Ks} component that is implicated in the work investigating the role of I_K in Wenckebach rhythms in guinea pig ventricular cells (11, 12). An E-4031-sensitive, rectifying component of I_K, similar in some respects to I_{Kr} in the guinea pig, has been identified in rabbit ventricular cells (6, 10, 42). Although one of these reports states that a slower component is absent (6), a recent abstract reports a much slower I_{Ks}-like component (34). In addition, I_{Kr} in the rabbit has kinetics that are much slower than those of I_{Kr} in the guinea pig (6, 10, 42). For example, the time constant at 33–35°C for deactivation of I_{Kr} at −60 mV is ~60 ms in the guinea pig (35), whereas it is ~250 ms in the rabbit (10). At room temperature, the time constant for deactivation of I_{Kr} at the resting potential is very long in the rabbit, ~700 ms at −80 mV from ensemble averaging of single-channel recordings (42). It is thus conceivable

that not only the slower I_{Ks} component but also the faster I_{Kr} component might play a role in generating beat-to-beat increases in latency in rabbit ventricular cells. In addition, whereas the fully activated magnitude of I_{Kr} is similar in the rabbit and the guinea pig (~1 pA/pF) (10, 35), any remaining component of I_K, presumably I_{Ks}, is much smaller in the rabbit than in the guinea pig (10, 17, 35, 40, 41). Hence it will be difficult to provide firm experimental evidence for any particular mechanism underlying the beat-to-beat increments in latency in rabbit ventricular cells.

In fact, it is not clear whether the beat-to-beat increments in latency seen in rabbit cells were crucial to the generation of Wenckebach rhythm. Indeed, imagine a situation in which the action potential is truly all or none, with no graded time-dependent recovery of latency but rather an abrupt change from no latency (i.e., skipped beat) to a fixed latency as recovery interval is gradually increased. After a skipped beat, as APD increases as the cycle progresses (because of the presence of I_{to}), there would be no beat-to-beat change in latency, but when the APD crosses the critical value producing the minimum DI possible, there would be a skipped beat, after which another Wenckebach cycle would ensue. By inserting time-dependent recovery of latency back into this system, one would then see a beat-to-beat increase in latency that would not be, at root, the cause of the Wenckebach rhythm, but rather an epiphenomenon.

It is well known that I_{to} plays a major role in controlling APD in rabbit ventricular muscle (4, 17). We now implicate I_{to} as the main player generating the beat-to-beat increments in APD during a Wenckebach cycle in isolated rabbit ventricular cells. This current has been investigated in single cells isolated from many areas of the heart, including the sinoatrial node (13), atrium (9, 17), AV node (31, 33), Purkinje fiber (4), and ventricle (5, 7, 16, 17, 24, 29, 32, 36, 39–41). There are two components to the current, one Ca^{2+} dependent and the other Ca^{2+} independent (24, 29). The Ca^{2+}-dependent component is 4-AP insensitive, appears to be carried by Cl^-, and is influenced by Ca^{2+}-channel blockers and Ca^{2+} buffers (47). The presence of 5 mmol/l EGTA in the pipette solution minimized the contribution of this Ca^{2+}-sensitive component of transient outward current in our experiments (24, 47). Because the addition of 4-AP, a blocker of the Ca^{2+}-insensitive component, abolished the beat-to-beat increments in APD (Fig. 4), these increments were attributable to the Ca^{2+}-insensitive component, which we refer to as I_{to}. This current is carried mainly by K^+ and is believed to be more important in determining APD because of its larger magnitude and more pronounced rate dependence (4, 17, 24).

A critical characteristic of I_{to} necessary for the generation of beat-to-beat increments in APD during Wenckebach rhythms in rabbit ventricular cells is its relatively slow recovery from inactivation. In other species, I_{to} recovers more quickly; e.g., in isolated human ventricular cells at room temperature, 80% of the amplitude of I_{to} recovers within 100 ms (32). However, there is also a much slower component of recovery present, because the remaining 20% of current recovers with a time constant of ~4.4 s at −80 mV (32). In addition, the peak I_{to} elicited with clamp steps repetitively delivered at an interval of 2 s was >300 pA greater than when the steps were delivered at an interval of 1 s (see Fig. 6 of Ref. 32). Although our results in rabbit cells would suggest that this difference should be enough to influence APD to an extent that would produce Wenckebach rhythms in human ventricular myocytes, this conjecture can only be examined by further experimental work.

Periodic versus aperiodic Wenckebach rhythms. In single guinea pig cells, it has been argued that the beat-to-beat increase in latency produces a beat-to-beat shortening of recovery interval, which results in a dropped beat once the recovery interval becomes too short (11, 12). These cells apparently did not show any systematic increase in APD as the cycle progressed (12), presumably because of the absence of I_{to} (40). Rabbit ventricular cells also show increments in latency (Figs. 1*C* and 4*D*, *top*) similar to those seen in guinea pig cells stimulated with 10-ms pulses (e.g., Fig. 2*C* of Ref. 12). However, the more prominent concomitant beat-to-beat increase in APD (Figs. 1*B*; 4, *A* and *C*, *top*; and 5*A*) contributed much more to the resultant beat-to-beat decrease in recovery interval (compare Fig. 4, *C* and *D*, *top*). This beat-to-beat decrease was large enough that a periodic 3:2 rhythm could be maintained for several cycles at 34–36°C and was only occasionally disrupted by a 2:1 or 4:3 cycle.

In contrast, when I_{to} was blocked with 4-AP, we obtained either a direct transition to complete block or to an unstable aperiodic Wenckebach rhythm, which was somewhat reminiscent of Mobitz type II block in its lack of predictability (Fig. 4, *C* and *D*, *bottom*). These Wenckebach cycles resembled those seen in the guinea pig in that there was a beat-to-beat increment in latency (Fig. 4*D*, *bottom*) with apparently stochastic fluctuations in APD (Fig. 4*C*, *bottom*). In these aperiodic Wenckebach rhythms, it was clear that the recovery interval was no longer playing a central role in controlling the timing of skipped beats, because action potentials and skipped beats occurred over the same range of RTs (~95–105 ms). We surmise that membrane noise generated by single-channel stochastic gating was responsible for these stochastic rhythms (21). Whereas the presence of I_{to} was thus not necessary to obtain Wenckebach rhythms, the beat-to-beat increase in APD produced when I_{to} was present provided a "noise margin" that perhaps counteracts the noise-induced fluctuations generated in the absence of I_{to}.

Under control conditions it was more difficult to elicit a maintained 3:2 periodic Wenckebach rhythm at 22–24°C than at 34–36°C (we observed instead typically a mixture of 3:2 and 4:3 or 2:1 cycles). This can be explained by the fact that, at 34–36°C, the APD of the second action potential during a 3:2 cycle was within 3% of that seen during 1:1 rhythm (Fig. 1*D*), making

the likelihood of a third action potential of longer APD quite minimal. However, at 24–26°C, the duration of the second action potential did not reach the 1:1 range (Fig. 1*D*), and therefore it became possible for a third action potential of longer APD to occur, generating a 4:3 cycle. This can also be appreciated from Fig. 5*D*, which shows that by the third beat, the time course of the staircase waveform in r has effectively reached its asymptotic limit, rendering higher order (e.g., 5:4, 6:5) Wenckebach cycles quite unlikely in the presence of noise.

Ca^{2+} current potentiation and use-dependent 4-AP block. Two factors that must be considered in the interpretation of our experimental results are Ca^{2+} current potentiation and use-dependent 4-AP block.

Ca^{2+} current potentiation or facilitation is a phenomenon described in rabbit (26) and guinea pig (30) ventricular cells in which there is a gradual increase in the peak inward Ca^{2+} current elicited during repetitive voltage-clamp steps applied after a relatively long rest period. Should Ca^{2+} current potentiation occur in our experiments, one would expect that the second action potential after a skipped beat would have an APD longer than that of the first beat, because the Ca^{2+} current would be increased. However, no such systematic trends in APD are found in either guinea pig cells (11, 12) or rabbit cells under the influence of 4-AP (Fig. 4, *A* and *C*, *bottom*; see also Fig. 8 of Ref. 23). In addition, potentiation of the Ca^{2+} current was not seen in isolated rabbit ventricular cells when the interval between clamp steps was short, e.g., 500 ms at 33–35°C (see Fig. 10 of Ref. 29) or even 5,000 ms at 30°C (Fig. 5 of Ref. 26). Potentiation was only seen at much longer interstep intervals (tens or hundreds of seconds) (26).

Reverse use-dependent 4-AP block of I_{to}, in which there is greater block of I_{to} after a longer rest at hyperpolarized levels, has been described previously in dog ventricular muscle (39) as well as in isolated rat (7) and ferret (5) ventricular cells. If reverse use dependence were occurring in the AP clamp experiment in Fig. 5, one would thus expect the greatest degree of block of I_{to} during the first beat of the Wenckebach cycle, because it is preceded by the longest recovery interval. This would result in the clamp injecting a compensating current larger than that which it would inject in the absence of reverse use-dependent block, which would then manifest as an apparent increase in I_{to} amplitude on the first beat of the cycle. As the Wenckebach cycle progresses, the beat-to-beat decrease in recovery interval would produce a beat-to-beat decrease in the degree of block, which would show up in the AP clamp current trace as an artifactual beat-to-beat decrease in I_{to}.

We offer three lines of evidence that use-dependent block does not contribute to our experimental results. First, we carried out voltage-clamp experiments in which we imposed a train of steps mimicking the beat-to-beat changes in APD that occur during a 4:3 Wenckebach cycle at BCL = 1,000 ms at 22–24°C (Fig. 5, *A* and *D*): a 200-ms step from −80 mV to +60 mV, followed by steps to −80 mV for 800 ms, +60 mV for 220 ms, −80 mV for 780 ms, +60 mV for 240 ms, and finally −80 mV for 1,760 ms. Although there was a beat-to-beat decrease in I_{to} during control, as in the corresponding AP clamp experiment (Fig. 5*B*), there was no I_{to} elicited by any of the three steps to +60 mV once 2 mmol/l 4-AP was added. Similar results were seen in five other cells. Second, the I_{to} waveform seen in our ionic model (Fig. 5*C*), which was based on data taken from independently conducted voltage-clamp experiments in which 4-AP was not involved, was very similar to that seen in our AP clamp experiments (Fig. 5*B*). Third, the APD remains quite constant when skipped-beat cycles were produced in the presence of 4-AP (Fig. 4, *A* and *C*, *bottom*). This could be caused by either a complete block of I_{to} or an exactly equal balance between the beat-to-beat increase in I_{to} caused by reverse use-dependent unblock and the beat-to-beat decrease in I_{to} caused by inactivation. We consider the latter possibility to be unlikely.

Although we argue above that use dependence of 2 mmol/l 4-AP did not play a role in our experiments, this does not rule out such effects in general. For example, in ferret ventricular myocytes at room temperature, in which the time course of recovery from inactivation of I_{to} is much faster than in rabbit cells at the same temperature, the time constant of unblock is much longer than the time constant of recovery from inactivation (5). In that case, one might expect to encounter effects caused by use dependence should a concentration of 4-AP be used that would leave some residual I_{to}.

Implications for AV Wenckebach block. Although Wenckebach block classically occurs at the AV node, it has been described clinically in virtually all areas of the heart, including infranodal structures (2, 15). Over the last century, many mechanisms have been proposed to account for Wenckebach AV block (19, 44). Perhaps the most commonly accepted mechanism is decremental conduction, in which the action potential that is eventually blocked gradually dies out as the AV node is traversed. The beat-to-beat increases in APD that can be seen during nodal Wenckebach are usually attributed to retrograde electrotonic injection of current from more distal areas of the node that are activated in a delayed fashion (19). However, recent voltage-clamp experiments reveal that I_{to} is present in 93% of rod-shaped and 42% of ovoid AV nodal cells (31), and the time constant of recovery from inactivation of I_{to} is on the order of seconds at 32–36°C in these cells (33). On the other hand, the beat-to-beat increase in latency and beat-to-beat decrease in maximal upstroke velocity in isolated AV nodal cells (1, 25) would probably be associated with a beat-to-beat slowing of conduction velocity through the node. Thus it may well be that there is no single ionic mechanism that, by itself, can account for the origin of Wenckebach block in the AV node. Although it is possible that a mechanism similar to that which we have described in isolated rabbit ventricular cells might be playing a role in generating Wenckebach block in the intact AV node, only further experimental work can investigate this hypothesis.

APPENDIX

The transient outward current was modeled with the expression

$$I_{to} = \bar{g}_{to} q r (V - E_{rev}) \quad (1)$$

where I_{to} is measured in pA, $\bar{g}_{to}$ is the maximal conductance (nS), q and r are the activation and inactivation variables, respectively, V is the transmembrane potential (mV), and E_{rev} is the reversal potential (mV). We set $\bar{g}_{to}$ to a value of 5.6 nS, which gives a peak I_{to} amplitude corresponding to that seen in our experiments at room temperature. This value is also within the range of prior estimates (9, 17). We set E_{rev} to −66 mV (9). The equation governing q is

$$dq/dt = (q_\infty - q)/\tau_q \quad (2)$$

where $q_\infty = [1 + \exp[-(V + 12.3)/18.2]]^{-1}$ from prior work on isolated rabbit ventricular cells (24). We set $\tau_q = 5$ ms on the basis of our experimental observations (see also Ref. 41). We use two separate formulas to describe the evolution of r, because inactivation and recovery from inactivation of I_{to} are different processes. For the recovery from inactivation

$$dr/dt = (r_\infty - r)/\tau_r \quad (3)$$

with $r_\infty = [1 + \exp[(V + 38.2)/9.8]]^{-1}$ from prior work (24). The extremely long time constant $\tau_r = 6.5$ s is taken from a voltage-clamp experiment in the same cell as that in which the AP clamp experiment of Fig. 5, *A* and *B*, was carried out and is in agreement with the value of 5.7 s previously reported at room temperature (17). In contrast to activation and removal of inactivation, the inactivation process has two time constants (9, 24), τ_{r1} and τ_{r2}, with the following time course during voltage clamp

$$r(t) = Ae^{-t/\tau_{r1}} + Be^{-t/\tau_{r2}} + r_\infty \quad (4)$$

where A and B are constants depending on initial conditions.

The differential equation that gives *Eq. 4* as its general solution is

$$d^2r/dt^2 = [(1/\tau_{r1}) + (1/\tau_{r2})]dr/dt] + [(r_\infty - r)/(\tau_{r1}\tau_{r2})] \quad (5)$$

We used Euler integration to numerically integrate *Eqs. 2*, *3*, and *5* with a fixed time step (Δt) of 1 ms, because the sampling frequency for the imposed AP clamp waveform in Fig. 5*A* was 1 kHz. Using the finite-difference approximation $[q(t) - q(t - \Delta t)]/\Delta t$ for dq/dt in *Eq. 2*, one obtains

$$q(t + \Delta t) = q_\infty - [q_\infty - q(t)]e^{-\Delta t/\tau_q} \quad (6a)$$

where q_∞ is evaluated at $V(t + \Delta t)$. During recovery from inactivation, one has from *Eq. 3*

$$r(t + \Delta t) = r_\infty - [r_\infty - r(t)]e^{-\Delta t/\tau_{tr}} \quad (6b)$$

where r_∞ is also evaluated at $V(t + \Delta t)$. During inactivation, using $[r(t) - r(t - \Delta t)]/\Delta t$ for dr/dt and $[r(t + \Delta t) - 2r(t) + r(t - \Delta t)]/(\Delta t)^2$ for d^2r/d^2t in *Eq. 5*, one obtains

$$r(t + \Delta t) = \frac{r(t)\left[\frac{2}{(\Delta t)^2} + \left(\frac{\tau_{r1} + \tau_{r2}}{\tau_{r1}\tau_{r2}}\right)\frac{1}{\Delta t} - \frac{1}{\tau_{r1}\tau_{r2}}\right] - \frac{r(t - \Delta t)}{(\Delta t)^2} + \frac{r_\infty}{\tau_{r1}\tau_{r2}}}{\frac{1}{(\Delta t)^2} + \left(\frac{\tau_{r1} + \tau_{r2}}{\tau_{r1}\tau_{r2}}\right)\frac{1}{\Delta t}} \quad (6c)$$

where again r_∞ is evaluated at $V(t + \Delta t)$. We thus use *Eq. 6c* during the time that r is decreasing (i.e., inactivation is proceeding) and *Eq. 6b* while r is increasing (i.e., recovery from inactivation is proceeding). For the simulation of Fig. 5, *C* and *D*, the values $\tau_{r1} = 40$ ms, $\tau_{r2} = 318$ ms, and $A/(A + B) = 0.4$ used in *Eq. 4* were obtained from a voltage-clamp step from −80 mV to +60 mV in this same cell and are in accord with previous results (17). Initial conditions [$q(0) = 0.00874$, $r(0) = 0.12417$] are chosen so as to be close to "on-cycle" initial conditions; i.e., q and r at $t = 4$ s equal q and r at $t = 0$, respectively.

We thank F. Alonso, D. Jeandupeux, and A. Ogbaghebriel for help in the early phase of the experimental work. We also thank C. Gordon for expert technical assistance in isolating cells and Adam Sherman for making available the Patchkit program.

This work was supported by a Heart and Stroke Foundation of Quebec Grant-in-Aid (to M. Guevara) and a Medical Research Council of Canada operating grant (to A. Shrier). A. Yehia was supported by a Fonds pour la Formation de Chercheurs et d'Aide à la Recherche team grant. K. Lo received a Fonds de la Recherche en Santé du Québec summer undergraduate research award.

Address for reprint requests: A. Yehia, Dept. of Physiology, McGill Univ., 3655 Drummond St., Montreal, Quebec, Canada H3G 1Y6.

Received 4 October 1996; accepted in final form 14 February 1997.

REFERENCES

1. **Adjemian, R., M. R. Guevara, and A. Shrier.** Wenckebach rhythms and ionic currents in rabbit atrioventricular nodal cells (Abstract). *Biophys. J.* 59: 465a, 1991.
2. **Anderson, G. J., K. Greenspan, and C. Fisch.** Electrophysiologic studies on Wenckebach structures below the atrioventricular junction. *Am. J. Cardiol.* 30: 232–236, 1972.
3. **Anumonwo, J. M. B., M. Delmar, A. Vinet, D. C. Michaels, and J. Jalife.** Phase resetting and entrainment of pacemaker activity in single sinus nodal cells. *Circ. Res.* 68: 1138–1153, 1991.
4. **Binah, O.** The transient outward current in the mammalian heart. In: *Cardiac Electrophysiology: A Textbook*, edited by M. R. Rosen, M. J. Janse, and A. L. Wit. Mount Kisco, NY: Futura, 1990, p. 93–105.
5. **Campbell, D. L., Y. Qu, R. L. Rasmusson, and H. C. Strauss.** The calcium-independent transient outward potassium current in isolated ferret right ventricular myocytes. II. Closed state reverse use-dependent block by 4-aminopyridine. *J. Gen. Physiol.* 101: 603–626, 1993.
6. **Carmeliet, E.** Use-dependent block and use-dependent unblock of the delayed rectifier K^+ current by almokalant in rabbit ventricular myocytes. *Circ. Res.* 73: 857–868, 1993.
7. **Castle, N. A., and M. T. Slawsky.** Characterization of 4-aminopyridine block of the transient outward K^+ current in adult rat ventricular myocytes. *J. Pharmacol. Exp. Ther.* 264: 1450–1459, 1992.
8. **Chialvo, D. R., and J. Jalife.** Non-linear dynamics of cardiac excitation and impulse propagation. *Nature* 330: 749–752, 1987.
9. **Clark, R. B., W. R. Giles, and Y. Imaizumi.** Properties of the transient outward current in rabbit atrial cells. *J. Physiol. (Lond.)* 405: 147–168, 1988.
10. **Clay, J. R., A. Ogbaghebriel, T. Paquette, B. I. Sasyniuk, and A. Shrier.** A quantitative description of E-4031-sensitive repolarization current in rabbit ventricular myocytes. *Biophys. J.* 69: 1830–1837, 1995.
11. **Delmar, M., L. Glass, D. C. Michaels, and J. Jalife.** Ionic basis and analytical solution of the Wenckebach phenomenon in guinea pig ventricular myocytes. *Circ. Res.* 65: 775–788, 1989.
12. **Delmar, M., D. C. Michaels, and J. Jalife.** Slow recovery of excitability and the Wenckebach phenomenon in the single guinea pig ventricular myocyte. *Circ. Res.* 65: 761–774, 1989.
13. **Denyer, J. C., and H. F. Brown.** Rabbit sino-atrial node cells: isolation and electrophysiological properties. *J. Physiol. (Lond.)* 428: 405–424, 1990.

14. **Doerr, T., R. Denger, A. Doerr, and W. Trautwein.** Ionic currents contributing to the action potential in single ventricular myocytes of the guinea pig studied with action potential clamp. *Pflügers Arch.* 416: 230–237, 1990.
15. **Downar, E., and M. B. Waxman.** Depressed conduction and unidirectional block in Purkinje fibres. In: *The Conduction System of the Heart*, edited by H. J. J. Wellens, K. I. Lie, and M. J. Janse. Philadelphia, PA: Lea and Febiger, 1976, p. 393–409.
16. **Fedida, D., and W. R. Giles.** Regional variations in action potentials and transient outward current in myocytes isolated from rabbit left ventricle. *J. Physiol. (Lond.)* 442: 191–209, 1991.
17. **Giles, W. R., and Y. Imaizumi.** Comparison of potassium currents in rabbit atrial and ventricular cells. *J. Physiol. (Lond.)* 405: 123–145, 1988.
18. **Guevara, M. R.** *Chaotic Cardiac Dynamics* (PhD thesis). Montreal, Canada: McGill University, 1984.
19. **Guevara, M. R.** Spatiotemporal patterns of block in an ionic model of cardiac Purkinje fibre. In: *From Chemical to Biological Organization*, edited by M. Markus, S. C. Müller, and G. Nicolis. Berlin: Springer-Verlag, 1988, p. 273–281.
20. **Guevara, M. R., D. Jeandupeux, F. Alonso, and N. Morissette.** Wenckebach rhythms in isolated ventricular heart cells. In: *International Conference on Singular Behaviour and Nonlinear Dynamics*, edited by S. Pnevmatikos, T. Bountis, and S. Pnevmatikos. Singapore: World Scientific, 1989, vol. 2, p. 629–642.
21. **Guevara, M. R., and T. J. Lewis.** A minimal single-channel model for the regularity of beating in the sinoatrial node. *Chaos* 5: 174–183, 1995.
22. **Guevara, M. R., A. Shrier, and L. Glass.** Phase-locked rhythms in periodically stimulated heart cell aggregates. *Am. J. Physiol.* 254 (*Heart Circ. Physiol.* 23): H1–H10, 1988.
23. **Hiraoka, M., and S. Kawano.** Mechanism of increased amplitude and duration of the plateau with sudden shortening of diastolic intervals in rabbit ventricular cells. *Circ. Res.* 60: 14–26, 1987.
24. **Hiraoka, M., and S. Kawano.** Calcium-sensitive and insensitive transient outward current in rabbit ventricular myocytes. *J. Physiol. (Lond.)* 410: 187–212, 1989.
25. **Hoshino, K., J. Anumonwo, M. Delmar, and J. Jalife.** Wenckebach periodicity in single atrioventricular nodal cells from the rabbit heart. *Circulation* 82: 2201–2216, 1990.
26. **Hryshko, L. V., and D. M. Bers.** Ca current facilitation during postrest recovery depends on Ca entry. *Am. J. Physiol.* 259 (*Heart Circ. Physiol.* 28): H951–H961, 1990.
27. **Ibarra, J., G. E. Morley, and M. Delmar.** Dynamics of the inward rectifier K^+ current during the action potential of guinea pig ventricular myocytes. *Biophys. J.* 60: 1534–1539, 1991.
28. **Isenberg, G., and U. Klockner.** Calcium tolerant ventricular myocytes prepared by pre-incubation in a "KB medium." *Pflügers Arch.* 395: 6–18, 1982.
29. **Kawano, S., and M. Hiraoka.** Transient outward currents and action potential alterations in rabbit ventricular myocytes. *J. Mol. Cell. Cardiol.* 23: 681–693, 1991.
30. **Lee, K. S.** Potentiation of the calcium-channel currents of internally perfused mammalian heart cells by repetitive depolarization. *Proc. Natl. Acad. Sci. USA* 84: 3941–3945, 1987.
31. **Munk, A. A., R. A. Adjemian, J. Zhao, A. Ogbaghebriel, and A. Shrier.** Electrophysiological properties of morphologically distinct cells isolated from the rabbit atrioventricular node. *J. Physiol. (Lond.)* 493: 801–818, 1996.
32. **Näbauer, M., D. J. Beuckelmann, and E. Erdmann.** Characteristics of transient outward current in human ventricular myocytes from patients with terminal heart failure. *Circ. Res.* 73: 386–394, 1993.
33. **Nakayama, T., and H. Irisawa.** Transient outward current carried by potassium and sodium in quiescent atrioventricular node cells of rabbits. *Circ. Res.* 57: 65–73, 1985.
34. **Salata, J. J., N. K. Jurkiewicz, B. Jow, P. J. Guinosso, Jr., and B. Fermini.** Evidence for the slowly-activating component of the delayed rectifier K^+ current (I_{Ks}) in rabbit ventricular myocytes (Abstract). *Biophys. J.* 68: a147, 1995.
35. **Sanguinetti, M. C., and N. K. Jurkiewicz.** Two components of cardiac delayed rectifier K^+ currents: differential sensitivity to block by class III antiarrhythmic agents. *J. Gen. Physiol.* 96: 195–215, 1990.
36. **Saxon, M. E., and V. G. Safronova.** The rest-dependent depression of action potential duration in rabbit myocardium and the possible role of the transient outward current. A pharmacological analysis. *J. Physiol. Paris* 78: 461–466, 1982.
37. **Shimoni, Y., R. B. Clark, and W. R. Giles.** Role on an inwardly rectifying potassium current in rabbit ventricular action potential. *J. Physiol. (Lond.)* 448: 709–727, 1992.
38. **Shrier, A., H. Dubarsky, M. Rosengarten, M. R. Guevara, S. Nattel, and L. Glass.** Prediction of complex atrioventricular conduction rhythms in humans with use of the atrioventricular nodal recovery curve. *Circulation* 76: 1196–1205, 1987.
39. **Simurda, J., M. Simurdova, and G. Christé.** Use-dependent effects of 4-aminopyridine on transient outward current in dog ventricle muscle. *Pflügers Arch.* 415: 244–246, 1989.
40. **Varró, A., D. A. Lathrop, S. B. Hester, P. P. Nánási, and J. G. Y. Papp.** Ionic currents and action potentials in rabbit, rat, and guinea pig ventricular myocytes. *Basic Res. Cardiol.* 88: 93–102, 1993.
41. **Varró, A., P. P. Nánási, and D. A. Lathrop.** Voltage-clamp characteristics of ventricular myocytes in rabbit. *Cardioscience* 2: 233–243, 1991.
42. **Veldkamp, M. W., A. C. G. van Ginneken, and L. N. Bouman.** Single delayed rectifier channels in the membrane of rabbit ventricular myocytes. *Circ. Res.* 72: 865–878, 1993.
43. **Watanabe, T., P. M. Rautaharju, and T. F. McDonald.** Ventricular action potentials, ventricular extracellular potentials, and the ECG of guinea pig. *Circ. Res.* 57: 362–373, 1985.
44. **Watanabe, Y., and L. S. Dreifus.** Second degree atrioventricular block. *Cardiovasc. Res.* 1: 150–158, 1967.
45. **Wenckebach, K. F.** Zur Analyse des unregelmässigen Pulses. II. Ueber den regelmässig intermittirenden Puls. *Z. Klin. Med. (Berl.)* 37: 475–488, 1899.
46. **Yehia, A., A. Shrier, and M. Guevara.** Transient outward current contributes to Wenckebach type action potential patterns in isolated ventricular myocytes (Abstract). *Proc. Int. Congr. Physiol. Sci. 32nd Glasgow 1993*, vol. 18, p. 139.49/P.
47. **Zygmunt, A. C., and W. R. Gibbons.** Calcium-activated chloride current in rabbit ventricular myocytes. *Circ. Res.* 68: 424–437, 1991.